Synthesis and Characterization of New Dinuclear Complexes $(CO)_5MnRe(CO)_3(L)$ (L = 2,2′-Bipyrimidine, 2,3-Bis(2-pyridyl)pyrazine) and Trinuclear Compounds $(CO)_5MnRe(CO)_3(L)R$ (R = $Re(Br)(CO)_3$, $W(CO)_4$). Evidence for Asymmetric Distortion of the Bridging 2,2′-Bipyrimidine Ligand (L) in $(CO)_5MnRe(CO)_3(L)Re(Br)(CO)_3$ from the Crystal Structure and ^{1}H-NMR and Resonance Raman Spectra

J. W. M. van Outersterp and D. J. Stufkens*

Anorganisch Chemisch Laboratorium, Universiteit van Amsterdam, J. H. van't Hoff Research Institute, Nieuwe Achtergracht 166, 1018 WV Amsterdam, The Netherlands

J. Fraanje and K. Goubitz

Laboratorium voor Kristallografie, Universiteit van Amsterdam, Amsterdam Institute of Molecular Studies, Nieuwe Achtergracht 166, 1018 WV Amsterdam, The Netherlands

A. Vlček, Jr.*

J. Heyrovský Institute of Physical Chemistry, Academy of Sciences of the Czech Republic, Dolejškova 3, 182 23 Prague, Czech Republic

Received December 21, 1994[⊗]

This article describes the synthesis and spectroscopic (^{1}H-NMR, UV/vis, resonance Raman) properties of the new complexes $(CO)_5MnRe(CO)_3(L)$, $(CO)_5MnRe(CO)_3(L)Re(Br)(CO)_3$ (L = 2,2′-bipyrimidine (BPYM), 2,3-bis(2-pyridyl)pyrazine (DPP)), and $(CO)_5MnRe(CO)_3(BPYM)W(CO)_4$ and the single-crystal X-ray structure of $(CO)_5MnRe(CO)_3(BPYM)Re(Br)(CO)_3$. The crystals are triclinic, space group $P\bar{1}$, with cell dimensions a = 11.819(3) Å, b = 14.957(9) Å, c = 15.792(7) Å, α = 64.09(4)°, β = 88.88(7)°, γ = 88.22(8)°, and Z = 4. Least-squares refinement on F, for 4620 observed reflections, converged to R = 0.127. The two different metal fragments $(CO)_5MnRe(CO)_3$ and $Re(Br)(CO)_3$ are coordinated to BPYM via Re with $Mn(CO)_5$ and Br^- in a mutually trans position perpendicular to the BPYM plane. An important aspect of this structure is the asymmetric bonding within the bridging BPYM ligand. From the C−N bonds connected to the inter-ring C−C bond, those involving N atoms coordinated to the Re^0 atom of the $(CO)_5MnRe(CO)_3$ moiety are longer than those involving the N atoms coordinated to the Re^I atom of the $Re(Br)(CO)_3$ fragment. This asymmetry of BPYM is also evident from the ^{1}H-NMR spectrum and is responsible for the occurrence of two absorption bands in the visible region belonging to separate transitions from the two metal fragments to BPYM. It even manifests itself in the resonance Raman spectra by showing resonance enhancement of intensity for BPYM vibrations with slightly different frequencies upon excitation into either of these MLCT bands. This asymmetry is not observed for the corresponding DPP-bridged complex and also not for $(CO)_5MnRe(CO)_3(BPYM)W(CO)_4$. The resonance Raman spectra of the latter compound point to a reversal of the order of the a_u and b_{2u} π^* orbitals of BPYM as compared with the free ligand. The distortion of the BPYM ligand appears to be responsible for a very weak electronic π interaction between the two metal fragments in $(CO)_5MnRe(CO)_3(BPYM)Re(Br)(CO)_3$ which may thus be viewed as a mixed-valence complex.

Introduction

There is currently much interest[1] in spectroscopic, photophysical, and photochemical properties of multicomponent photoactive systems in which chromophoric, emissive, and/or photoreactive transition metal complexes are linked together by suitable bridging ligands, usually nitrogen-containing aromatic heterocycles.[2] Excitation of the chromophoric group(s) of these "supramolecules" is often followed by a cascade of intramolecular electron- or energy-transfer steps that determine the overall photoactivity, i.e. emission or reactivity. This behavior is strongly dependent on the nature of the bridging ligand, especially on its ability to mediate electronic communication between the metal atoms, in both the ground and electronically excited states of the polynuclear complexes. Moreover, bridging ligands with sufficiently low-lying π^* orbitals may become part of the chromophore, being directly involved in MLCT electronic transitions. Elucidation of the properties of bridging diimine ligands, namely their ability to transmit electronic effects between the bridged metals, is thus of paramount importance for the understanding, design, and possible exploitation of photoactive polynuclear complexes.

We have now extended our previous studies[3-7] on $(CO)_5MnRe(CO)_3$(α-diimine) complexes to trinuclear complexes of

* To whom correspondence should be addressed.

[⊗] Abstract published in *Advance ACS Abstracts*, August 1, 1995.

(1) Balzani, V.; Scandola, F. *Supramolecular Photochemistry*; Ellis Horwood Limited: Chichester, U.K., 1991.

(2) Steel, P. J. *Coord. Chem. Rev.* **1990**, *106*, 227.

(3) Kokkes, M. W.; Stufkens, D. J.; Oskam, A. *Inorg. Chem.* **1985**, *24*, 2934.

0020-1669/95/1334-4756$09.00/0

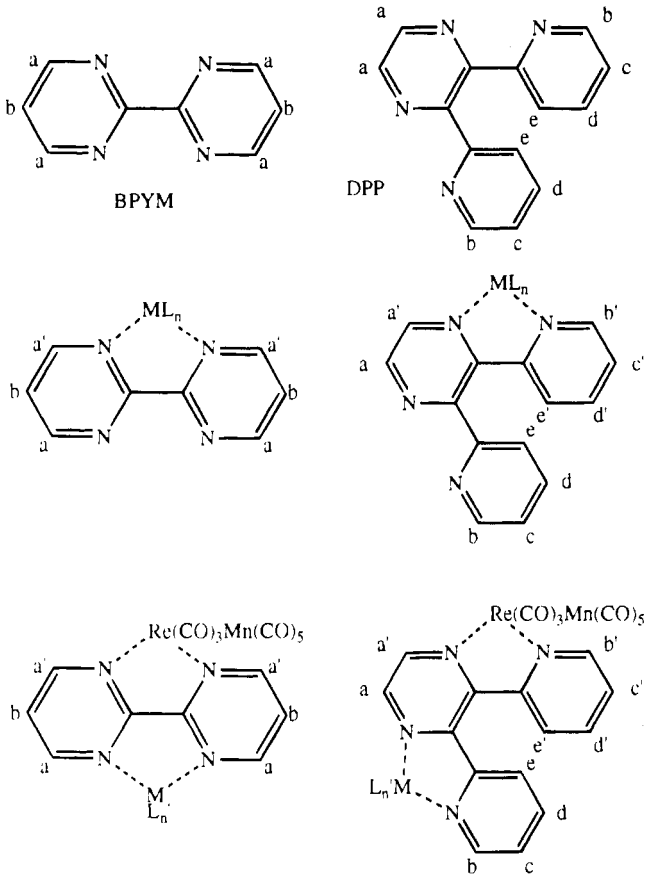

Figure 1. Schematic drawings of the bridging ligands BPYM and DPP (L), the mononuclear complexes $Re(Cl)(CO)_3(L)$, the dinuclear complexes $(CO)_5MnRe(CO)_3(L)$ (ML_n = $Re(Cl)(CO)_3$, $(CO)_5MnRe(CO)_3$) and the trinuclear complexes $(CO)_5MnRe(CO)_3(L)Re(Br)(CO)_3$, and $(CO)_5MnRe(CO)_3(BPYM)W(CO)_4$ (ML'_n = $Re(Br)(CO)_3$, $W(CO)_4$).

the type $(CO)_5MnRe(CO)_3(L)ML'_n$ (L = 2,2′-bipyrimidine (BPYM), 2,3-bis(2-pyridyl)pyrazine (DPP); ML'_n = $Re(Br)(CO)_3$, $W(CO)_4$) (Figure 1). To our knowledge, these complexes are the first examples of polynuclear species in which two metal atoms are linked by a direct Mn−Re covalent bond, and the other metal-containing fragment is separated from the dinuclear moiety by a bridging diimine ligand. As the metal-to-bridging ligand electronic transitions may occur from both the dinuclear and mononuclear metal fragment, these complexes may be regarded as bichromophores. Moreover, the $(CO)_5MnRe(CO)_3(L)$ moiety is potentially photoreactive with respect to Mn−Re bond homolysis.[3-6] Hence, these trinuclear complexes offer a unique possibility to study the ligand-mediated mutual influence of the metal-containing fragments on their spectroscopic and, for the dinuclear fragment, photochemical properties. The two bridging diimines used, BPYM and DPP, are very versatile ligands,[8-28] widely used to construct supramolecular transition metal compounds. However, their ground- and excited-state electronic properties are still not well understood and their ability to mediate electronic communication between metal atoms is also a subject of some controversy in the literature.[21,23,26] Moreover, a recent resonance Raman study[27] together with EPR results[28] pointed to the unusual, but important, role of the second lowest unoccupied orbital (SLUMO) of the BPYM ligand.

Aiming at understanding the nature of MLCT transitions to the bridging BPYM and DPP ligands and their role in electronically excited polynuclear complexes, we have investigated the electronic absorption and resonance Raman spectra of the trinuclear complexes $(CO)_5MnRe(CO)_3(L)ML'_n$ and compared them with the spectra of the dinuclear parent compounds, $(CO)_5MnRe(CO)_3(L)$ (L = BPYM, DPP). Moreover, the ^{1}H-NMR spectra of $(CO)_5MnRe(CO)_3(L)ML'_n$ and $(CO)_5MnRe(CO)_3(L)$ and the molecular structure of $(CO)_5MnRe(CO)_3(BPYM)Re(Br)(CO)_3$ were studied in order to better understand the influence of the metal fragments on the structure of the bridging ligands. Throughout this article the dinuclear complexes $(CO)_5MnRe(CO)_3(L)$ will be denoted as MnRe/L, and the trinuclear compounds $(CO)_5MnRe(CO)_3(L)Re(Br)(CO)_3$ and $(CO)_5MnRe(CO)_3(BPYM)W(CO)_4$ as MnRe/L/Re and MnRe/BPYM/W, respectively.

Experimental Section

Materials. THF, hexane, and toluene were freshly distilled from Na wire under N_2 prior to use. Acetonitrile was freshly distilled from P_2O_5 under N_2 before use. Diethyl ether was distilled under nitrogen from $CaCl_2$. The KNO_3 used for the Raman measurements was dried at 100 °C for at least 1 week. $Re_2(CO)_{10}$ and BPYM (Johnson & Matthey) and DPP (Merck) were used as received. The Silica 60 (MERCK) used for purification of the complexes was activated by heating overnight under vacuum at 180 °C and stored under nitrogen.

Spectroscopic Measurements. IR spectra were recorded either on a Nicolet 7199 B FTIR spectrometer using a liquid-nitrogen-cooled MCT detector (resolution 1.0 cm^{-1}) or on a BioRad FTS-7 FTIR spectrometer (resolution 2 cm^{-1}). Electronic absorption spectra were measured either on a Perkin-Elmer Lambda 5 UV/vis spectrophotometer connected to a 3600 data station or on a Varian Cary 4E spectrophotometer. ^{1}H-NMR spectra were recorded on a Bruker AC 100 or Bruker AMX 300 spectrometer. Resonance Raman studies were performed using a Dilor Modular XY system with a multichannel diode array detection system. The Raman spectra of the trinuclear compounds were taken from rotating KNO_3 pellets of the complexes at room temperature

(4) Kokkes, M. W.; Stufkens, D. J.; Oskam, A. *Inorg. Chem.* **1985**, *24*, 4411.
(5) Kokkes, M. W.; de Lange, W. G. J.; Stufkens, D. J.; Oskam, A. *J. Organomet. Chem.* **1985**, *294*, 59.
(6) Van der Graaf, T.; van Rooy, A.; Stufkens, D. J.; Oskam, A. *Inorg. Chim. Acta* **1991**, *187*, 133.
(7) Staal, L. H.; van Koten, G.; Vrieze, K. *J. Organomet. Chem.* **1979**, *175*, 73.
(8) Sahai, R.; Rillema, D. P.; Shaver, R.; van Wallendael, S.; Jackman, D. C.; Boldaji, M. *Inorg. Chem.* **1989**, *28*, 1022.
(9) Kaim, W.; Kohlmann, S. *Inorg. Chem.* **1987**, *26*, 68.
(10) Petersen, J. D. In *Photochemistry and Photophysics of Coordination Compounds*; Yersin, H., Vogler, A., Eds.; Springer-Verlag: Berlin, Heidelberg, 1987; p 147.
(11) Ruminski, R.; Cambron, R. T. *Inorg. Chem.* **1990**, *29*, 1575.
(12) Baiano, J. A.; Carlson, D. L.; Wolosh, G. M.; DeJesus, D. E.; Knowles, C. F.; Szabo, E. G.; Murphy, W. R., Jr. *Inorg. Chem.* **1990**, *29*, 2327.
(13) Winslow, L. N.; Rillema, D. P.; Welch, J. H.; Singh, P. *Inorg. Chem.* **1989**, *28*, 1596.
(14) Biedermann, J.; Gliemann, G.; Klement, U.; Range, K.-J.; Zabel, M. *Inorg. Chim. Acta* **1990**, *169*, 63.
(15) Buchanan, R. M.; Bauch, C.; Williams, D. E. *Acta Crystallogr.* **1989**, *C45*, 336.
(16) De Munno, G.; Bruno, G.; Julve, M.; Romeo, M. *Acta Crystallogr.* **1990**, *C46*, 1828.
(17) Matsubayashi, G.; Yamaguchi, Y.; Tanaka, T. *J. Chem. Soc., Dalton Trans.* **1988**, 2215.
(18) Van Wallendael, S.; Shaver, R. J.; Rillema, D. P.; Yoblinski, B. J.; Stathis, M.; Guarr, T. F. *Inorg. Chem.* **1990**, *29*, 1761.
(19) Overton, C.; Connor, J. A. *Polyhedron* **1982**, *1*, 53.
(20) Kalyanasundaram, K.; Nazeeruddin, M. K. *J. Chem. Soc., Dalton Trans.* **1990**, 1657.
(21) Brewer, K. J.; Murphy, W. R., Jr.; Petersen, J. D. *Inorg. Chem.* **1987**, *26*, 3376.
(22) Ruminski, R. R.; Petersen, J. D. *Inorg. Chem.* **1982**, *21*, 3706.
(23) Braunstein, C. H.; Baker, A. D.; Strekas, T. C.; Gafney, H. D. *Inorg. Chem.* **1984**, *23*, 857.
(24) Shoup, M.; Hall, B.; Ruminski, R. R. *Inorg. Chem.* **1988**, *27*, 200.
(25) Rillema, D. P.; Mack, K. B. *Inorg. Chem.* **1982**, *21*, 3849.
(26) MacQueen, D. B.; Petersen, J. D. *Inorg. Chem.* **1990**, *29*, 2313.
(27) Kaim, W.; Kohlmann, S.; Lees, A. J.; Snoeck, T. L.; Stufkens, D. J.; Zulu, M. M. *Inorg. Chim. Acta* **1993**, *210*, 159.
(28) (a) Matheis, W.; Kaim, W. *Inorg. Chim. Acta* **1991**, *181*, 15. (b) Matheis, W.; Kaim, W. Z. *Anorg. Allg. Chem.* **1991**, *593*, 147.

and excited by laser light whose wavelength was varied from 458 to 655 nm. For the wavelength range 458−514.5 nm, the lines of a SP Model 2016 argon ion laser were used. A Coherent CR 590 dye laser with Coumarin, Rhodamine B, or DCM dyes was used to cover the ranges 530−550, 560−610, and 620−655 nm, respectively. Elemental analyses were performed by the Microanalytisches Laboratorium of Dornis und Kolbe, Mülheim a.d. Ruhr, Germany.

Syntheses. MnRe/L. These complexes were prepared according to literature methods[7,29] from $Re(Br)(CO)_3(L)$[11,12] as starting material. The products were purified by column chromatography by elution with a gradient solution of THF and hexane. Anal. Found (calcd) for MnRe/BPYM: C, = 30.54 (30.82); H, 1.79 (0.96); N, = 7.31 (8.99). Found (calcd) for MnRe/DPP: C, 37.65 (37.77); H, 1.58 (1.43); N, 7.98 (8.01).

MnRe/L/Re. A solution of 1 mmol of MnRe/L and 1 mmol of $Re(Br)(CO)_3(CH_3CN)_2$[30] in THF was stirred overnight under nitrogen with the exclusion of light. The solution was evaporated to dryness, and the product was purified by column chromatography with THF and hexane as eluting solvents. MnRe/BPYM/Re was crystallized by diffusion of diethyl ether into a THF solution of the compound. A crystal structure was determined (see next section). For the DPP compound, no crystals could be obtained. Yields: 10−30%. Anal. Found (calcd) for MnRe/DPP/Re: C, 28.78 (28.60); H, 1.15 (0.95); N, 5.18 (5.33).

MnRe/BPYM/W. A 1 mmol sample of of $W(CO)_4(Me_3NO)_2$[31] and 1 mmol of MnRe/BPYM were stirred overnight under nitrogen in THF with the exclusion of light. The resulting solution was evaporated to dryness, and the product was purified by column chromatography with THF and hexane as the eluting solvents. Yield: 10−30%. Anal. Found (calcd) for MnRe/BPYM/W: C, 26.21 (26.12); H, 0.85 (0.65); N, 5.96 (6.09).

Crystal Structure Determination of MnRe/BPYM/Re. A dark green plate-shaped crystal with dimensions 0.03 × 0.20 × 0.20 mm, approximately, was used for data collection on an Enraf−Nonius CAD-4 diffractometer with graphite-monochromated Cu Kα radiation and $\omega-2\theta$ scan. A total of 6293 unique reflections were measured within the ranges $-12 \le h \le 12$, $-15 \le k \le 0$, $-16 \le l \le 15$. Of these, 4620 were above the significance level of $2.5\sigma(I)$. The maximum value of $(\sin\theta)/\lambda$ was 0.53 Å^{-1} ($3° < \theta < 55°$). Two reference reflections ($\bar{1}20$, 202) were measured hourly and showed no decrease during the 84 h collecting time. Unit-cell parameters were refined by a least-squares fitting procedure using 23 reflections with $71° \angle 2\theta \angle 82°$. Corrections for Lorentz and polarization effects were applied. The structure was solved by the PATTY/ORIENT/PHASEX option of the DIRDIF91 program system.[32] The hydrogen atoms were calculated and kept fixed at their calculated positions during the refinement with a fixed temperature factor of $U = 0.10$ Å^2. Full-matrix least-squares refinement on F, anisotropic for the Re and Mn atoms and isotropic for the remaining atoms, converged to $R = 0.127$, $R_w = 0.216$, $(\Delta/\sigma)_{max} = 0.04$. A weighting scheme $w = (7.9 + F_o + 0.0125F_o^2)^{-1}$ was used. An empirical absorption correction (DIFABS[33]) was applied, with coefficients in the range 0.69−2.06. A final difference Fourier map revealed a residual electron density between −4.2 and +5.7 e Å^{-3} in the vicinity of the heavy atoms. Scattering factors were taken from Cromer and Mann.[34] The anomalous scattering of Re, Mn, and Br was taken into account. The asymmetric unit contains two independent molecules. Matching both molecules, except for the hydrogen atoms, led to an RMS = 0.29 Å^2. All calculations were performed with XTAL,[35] unless stated otherwise.

The structure was extremely difficult to refine. The only way to refine the starting model, as obtained through DIRDIF, was as follows. The positions and (isotropic) temperature factors of the heavy atoms were refined as usual. However, the positions of the other non-hydrogen atoms were fixed at their model positions while their temperature factors were refined isotropically. Eventually, this refinement protocol converged to an R factor of 0.26. After the absorption correction was performed, the entire structure refinement was finished gradually in the normal way, refining simultaneously the positions of all atoms and the temperature factors of all non-hydrogen atoms. Attempts to refine all non-hydrogen atoms anisotropicaly failed; nearly half of those became not-positive definite. In order to maintain a chemically realistic model, it was necessary to couple some atoms with (soft) restraints, so their distances (and for the CO's also their angles) would remain at realistic values. The distances and angles for those restraints were taken from the literature. The rather high final R factor and the necessity of the special refinement protocol are probably due to the (poor) quality of the crystals, although the measurement did not indicate that. The experimental data for the crystal structure determination of MnRe/BPYM/Re are listed in Table 1.

Table 1. Crystallographic Data for MnRe/BPYM/Re

chem formula	$C_{19}H_6N_4O_{11}BrMnRe_2$
fw	973.5
space group	$P\bar{1}$
a, Å	11.819(3)
b, Å	14.957(9)
c, Å	15.792(7)
α, β, γ, deg	64.09(4), 88.88(7), 88.22(8)
V, Å^3	2510(4)
Z	4
d_{calc}, g cm^{-3}	2.58
λ(Cu Kα), Å	1.5418
μ(Cu Kα), cm^{-1}	243.2
F(000)	1784
T, K	293
R^a	0.127
$R_w{}^b$	0.216

$^a R = \sum||F_o| - k|F_c||/\sum|F_o|$. $^b R_w = \sum w(|F_o| - k|F_c|)^2/\sum w|F_o|^2$.

Results and Discussion

Syntheses of MnRe/L/Re and MnRe/BPYM/W. To our knowledge, this is the first time that complexes were prepared in which a photoreactive metal−metal−bonded fragment is linked to either a $Re(Br)(CO)_3$ or a $W(CO)_4$ fragment via a bridging ligand such as BPYM or DPP. The complexes are formed by substitution of the weakly coordinated CH_3CN and Me_3NO ligands in $Re(Br)(CO)_3(CH_3CN)_2$ and $W(CO)_4(Me_3NO)_2$, respectively, by the potentially bridging BPYM and DPP ligands of the MnRe/L complexes. As the complexes are photolabile, the syntheses had to be carried out in the dark. The products were purified by column chromatography.

X-ray Structure Determination of MnRe/BPYM/Re. The final positional parameters and the equivalent isotropic thermal parameters for the non-hydrogen atoms of the two independent molecules are given in Table 2. An ORTEP drawing of the crystal structure is presented in Figure 2. A selection of bond distances and bond angles is given in Tables 3 and 4, respectively. The two metal fragments $(CO)_5MnRe(CO)_3$ and $Re(Br)(CO)_3$ are bound to each other via the BPYM bridging ligand while the $(CO)_5MnRe(CO)_3$ moiety contains a Mn−Re metal−metal bond. All three metal atoms are coordinated in a slightly distorted octahedral geometry. The Re^0 (Re(1)) and Re^I (Re(2)) atoms are in the plane of the BPYM ligand. The $(CO)_5Mn$ fragment and the Br^- ion are in a perpendicular position with respect to this plane and in a trans position with respect to each other. The CO ligands of $Mn(CO)_5$ and $Re(CO)_3$(BPYM) are in a staggered position, just as for $Mn_2(CO)_{10}$[36] and $(CO)_5ReMn(CO)_3$(iPr-DAB).[37]

The average manganese−rhenium(1) bond length (2.99 Å)

(29) Morse, D. L.; Wrighton, M. S. *J. Am. Chem. Soc.* **1976**, *98*, 3931.
(30) Treichel, P. M.; Williams, J. P. *J. Organomet. Chem.* **1977**, *135*, 39.
(31) Koelle, U. *J. Organomet. Chem.* **1977**, *133*, 53.
(32) Smits, J. M. M.; Behm, H.; Bosman, W. P.; Beurskens, P. T. *J. Crystallogr. Spectrosc. Res.* **1991**, *18*, 447.
(33) Walker, N.; Stuart, D. *Acta Crystallogr.* **1983**, *A39*, 158.
(34) Cromer, D. T.; Mann, J. B. *Acta Crystallogr.* **1968**, *A24*, 321.
(35) Hall, S. R., Flack, H. D., Stewart, J. M., Eds. XTAL3.2 Reference Manual. Universities of Western Australia, Geneva, and Maryland, 1992.

Table 2. Fractional Coordinates and Isotropic Thermal Parameters ($Å^2$) with Estimated Standard Deviations in Parentheses

atom	*x*	*y*	*z*	U_{eq}
Re(1a)	0.7303(2)	0.0131(2)	0.7179(1)	0.039(1)
Re(2a)	0.2564(2)	−0.0895(2)	0.7271(2)	0.044(1)
Mn(1a)	0.7024(7)	0.1010(6)	0.8541(6)	0.050(5)
Br(1a)	0.3428(5)	−0.1455(5)	0.6050(4)	0.061(4)
C(1a)	0.638(4)	−0.193(3)	0.868(3)	0.04(1)[a]
C(2a)	0.566(5)	−0.261(5)	0.905(4)	0.06(2)[a]
C(3a)	0.446(4)	−0.240(2)	0.871(3)	0.04(1)[a]
C(4a)	0.497(2)	−0.087(3)	0.768(3)	0.04(1)[a]
C(5a)	0.551(4)	0.168(2)	0.575(3)	0.04(1)[a]
C(6a)	0.434(4)	0.193(3)	0.540(3)	0.04(1)[a]
C(7a)	0.362(4)	0.130(2)	0.584(2)	0.04(1)[a]
C(8a)	0.473(2)	0.014(2)	0.690(2)	0.025(9)[a]
C(9a)	0.829(3)	0.120(3)	0.642(3)	0.06(1)[a]
C(10a)	0.859(3)	−0.058(3)	0.793(3)	0.05(1)[a]
C(11a)	0.771(4)	−0.038(4)	0.628(3)	0.06(1)[a]
C(12a)	0.176(4)	−0.212(2)	0.792(3)	0.05(1)[a]
C(13a)	0.125(3)	−0.031(3)	0.649(3)	0.05(1)[a]
C(14a)	0.205(3)	−0.046(4)	0.822(3)	0.05(1)[a]
C(15a)	0.678(4)	0.157(5)	0.934(4)	0.08(2)[a]
C(16a)	0.667(6)	0.210(3)	0.749(3)	0.10(2)[a]
C(17a)	0.735(5)	−0.023(3)	0.939(3)	0.08(2)[a]
C(18a)	0.558(3)	0.068(4)	0.858(3)	0.07(2)[a]
C(19a)	0.851(3)	0.127(8)	0.840(5)	0.14(4)[a]
N(1a)	0.610(2)	−0.101(2)	0.794(3)	0.06(1)[a]
N(2a)	0.413(2)	−0.147(2)	0.803(2)	0.025(7)[a]
N(3a)	0.567(2)	0.075(2)	0.652(2)	0.05(1)[a]
N(4a)	0.369(2)	0.034(2)	0.658(2)	0.033(8)[a]
O(9a)	0.884(3)	0.185(3)	0.596(3)	0.08(1)[a]
O(10a)	0.936(3)	−0.103(3)	0.836(3)	0.07(1)[a]
O(11a)	0.782(3)	−0.071(3)	0.576(2)	0.07(1)[a]
O(12a)	0.126(3)	−0.283(2)	0.833(3)	0.07(1)[a]
O(13a)	0.050(3)	0.007(3)	0.602(3)	0.10(1)[a]
O(14a)	0.157(3)	−0.026(3)	0.874(3)	0.08(1)[a]
O(15a)	0.660(3)	0.192(3)	0.985(3)	0.07(1)[a]
O(16a)	0.641(4)	0.277(3)	0.679(2)	0.08(1)[a]
O(17a)	0.752(4)	−0.103(3)	0.998(3)	0.11(2)[a]
O(18a)	0.466(3)	0.045(4)	0.860(4)	0.11(2)[a]
O(19a)	0.946(3)	0.143(5)	0.832(4)	0.12(2)[a]
Re(1b)	−0.2546(2)	0.5232(2)	0.2414(2)	0.047(1)
Re(2b)	0.2252(2)	0.4442(2)	0.1970(2)	0.045(1)
Mn(1b)	−0.2052(9)	0.6039(7)	0.3802(6)	0.065(6)
Br(1b)	0.1562(6)	0.3873(5)	0.0743(4)	0.068(4)
C(1b)	−0.087(5)	0.687(3)	0.086(3)	0.06(1)[a]
C(2b)	0.009(5)	0.715(4)	0.050(4)	0.06(1)[a]
C(3b)	0.098(5)	0.657(3)	0.069(3)	0.06(1)[a]
C(4b)	−0.005(2)	0.536(3)	0.177(3)	0.05(1)[a]
C(5b)	−0.137(5)	0.313(3)	0.358(3)	0.06(1)[a]
C(6b)	−0.049(4)	0.249(4)	0.381(3)	0.05(1)[a]
C(7b)	0.057(4)	0.278(2)	0.340(3)	0.04(1)[a]
C(8b)	−0.013(2)	0.439(3)	0.248(3	0.04(1)[a]
C(9b)	−0.371(4)	0.447(3)	0.326(3)	0.06(1)[a]
C(10b)	−0.363(3)	0.632(2)	0.184(2)	0.022(8)[a]
C(11b)	−0.307(5)	0.474(3)	0.154(3)	0.06(1)[a]
C(12b)	0.353(3)	0.515(3)	0.121(3)	0.05(1)[a]
C(13b)	0.319(3)	0.327(2)	0.264(4)	0.06(1)[a]
C(14b)	0.255(3)	0.486(3)	0.297(2)	0.04(1)[a]
C(15b)	−0.165(5)	0.659(4)	0.456(3)	0.08(2)[a]
C(16b)	−0.206(4)	0.475(2)	0.464(4)	0.07(2)[a]
C(17b)	−0.212(6)	0.724(3)	0.281(3)	0.09(2)[a]
C(18b)	−0.061(3)	0.590(4)	0.348(3)	0.06(1)[a]
C(19b)	−0.356(2)	0.603(4)	0.397(3)	0.06(1)[a]
N(1b)	−0.106(2)	0.593(2)	0.162(2)	0.038(9)[a]
N(2b)	0.095(2)	0.560(2)	0.139(2)	0.05(1)[a]
N(3b)	−0.117(2)	0.411(2)	0.293(3)	0.07(1)[a]
N(4b)	0.073(2)	0.376(2)	0.274(2)	0.033(8)[a]
O(9b)	−0.440(4)	0.403(4)	0.378(3)	0.11(2)[a]
O(10b)	−0.431(3)	0.694(3)	0.155(3)	0.09(1)[a]
O(11b)	−0.338(3)	0.442(3)	0.105(3)	0.08(1)[a]
O(12b)	0.427(3)	0.560(3)	0.076(3)	0.09(1)[a]
O(13b)	0.380(3)	0.260(2)	0.302(3)	0.07(1)[a]
O(14b)	0.301(4)	0.503(4)	0.351(3)	0.11(2)[a]
O(15b)	−0.145(3)	0.690(3)	0.509(3)	0.07(1)[a]
O(16b)	−0.190(5)	0.394(3)	0.513(4)	0.12(2)[a]
O(17b)	−0.216(5)	0.802(3)	0.216(3)	0.11(2)[a]
O(18b)	0.033(3)	0.577(4)	0.339(3)	0.10(2)[a]
O(19b)	−0.453(3)	0.600(5)	0.412(4)	0.12(2)[a]

[a] Refined isotropically.

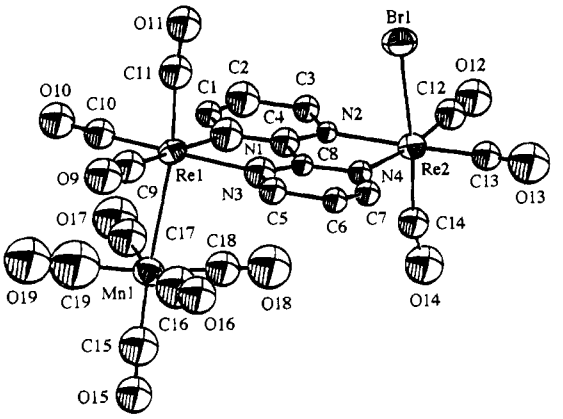

Figure 2. ORTEP drawing of the X-ray structure of MnRe/BPYM/Re.

is comparable with that in $(CO)_5ReMn(CO)_5$ (2.96 Å),[38] and the average length of the Re(2)−Br bond of 2.593 Å is comparable with that in $Re(Br)(CO)_3(DPP)$[39] (2.61 Å).

The BPYM ligand coordinates via σ(N(1)) and σ(N(3)) to the MnRe fragment and with σ(N(2)) and σ (N(4)) to the ReBr fragment. The average bite angles of 74.5 and 76.7°, respectively, which cause the deviation from a regular octahedral structure, were also found for other BPYM compounds,[14−17] as shown in Table 5. This table also presents the distances of the C−N bonds connected to the inter-ring C(4)−C(8) bond of MnRe/BPYM/Re and of several mononuclear BPYM complexes. The latter complexes all show a slight difference in bond distances between the coordinating (N(4)−C(8) and N(2)−C(4)) and noncoordinating part (N(3)−C(8) and N(1)−C(4)) of BPYM. This effect is, however, stronger when BPYM forms a bridge between metals in different oxidation states as we found for MnRe/BPYM/Re (see Figure 3). On the average, the C(4,8)−N bonds adjacent to the $(CO)_5MnRe^0(CO)_3$ fragment are 0.095 Å longer than those next to the $Re^I(Br)(CO)_3$ unit, compared with less than 0.02 Å for the mononuclear complexes. The average length of the C−N bonds adjacent to Re^0 is 1.400 Å; those adjacent to Re^I have an average bond distance of 1.305 Å. This difference in bond lengths agrees with the difference in π-back-bonding between Re^0 and Re^I that involves the b_{2u} bipyrimidine orbital which is strongly π-antibonding with respect to the C(4,8)−N bonds (vide infra; Figure 6). Hence, stronger π-back-donation from Re^0 results in longer C−N bonds within the $MnRe^0NCCN$ chelate ring, as compared with the Re^I side of the molecule. Other bonds within the pyrimidine rings are affected very little by the population of the b_{2u} orbital (Figure 6). Hence, neither the lengths of the N−C bonds which are not part of the chelate rings nor the observed alternations of the intra-ring C−C bonds depend on the oxidation states of the adjacent Re atoms. We are dealing here with a clear asymmetric distortion of BPYM which is also reflected in the ^{1}H-NMR, resonance Raman, and absorption spectra to be discussed hereafter.

^{1}H-NMR Spectra. The ^{1} H-NMR data for the di- and trinuclear complexes are listed in Table 6. As far as possible, the assignments were made by comparison with the ^{1}H-NMR spectra of analogous $Re(Cl)(CO)_3(L)Re(Cl)(CO)_3$ complexes.[18] The labels correspond to individual protons as indicated in Figure 1.

(36) Churchill, M. R.; Amon, K. N.; Wasserman, H. J. *Inorg. Chem.* **1981**, *20*, 1609.
(37) Kokkes, M. W.; Snoeck, T. L.; Stufkens, D. J.; Oskam, A.; Cristophersen, M.; Stam, C. H. *J. Mol. Struct.* **1985**, *131*, 11.
(38) Struchkov, Yu. T.; Anisimov, K. N.; Osipova, O. P.; Kolobova, N. E.; Nesmeyanov, A. N. *Dokl. Akad. Nauk. SSSR* **1967**, *172*, 107.
(39) van Outersterp, J. W. M.; et al. Unpublished results.

Table 3. Selected Bond Distances (Å) with Estimated Standard Deviations in Parentheses

Re(1a)−Mn(1a)	2.98(1)	Re(2a)−N(2a)	2.16(2)	C(3a)−N(2a)	1.39(4)
Re(1a)−C(9a)	1.93(4)	Re(2a)−N(4a)	2.18(2)	C(4a)−C(8a)	1.50(4)
Re(1a)−C(10a)	1.93(4)	Mn(1a)−C(15a)	1.81(8)	C(4a)−N(1a)	1.40(4)
Re(1a)−C(11a)	1.93(6)	Mn(1a)−C(16a)	1.79(4)	C(4a)−N(2a)	1.30(4)
Re(1a)−N(1a)	2.16(3)	Mn(1a)−C(17a)	1.79(3)	C(5a)−C(6a)	1.48(6)
Re(1a)−N(3a)	2.19(3)	Mn(1a)−C(18a)	1.78(4)	C(5a)−N(3a)	1.40(4)
Re(2a)−Br(1a)	2.598(8)	Mn(1a)−C(19a)	1.80(4)	C(6a)−C(7a)	1.25(5)
Re(2a)−C(12a)	1.93(3)	C(1a)−C(2a)	1.28(7)	C(7a)−N(4a)	1.40(3)
Re(2a)−C(13a)	1.93(3)	C(1a)−N(1a)	1.39(4)	C(8a)−N(3a)	1.40(4)
Re(2a)−C(14a)	1.95(6)	C(2a)−C(3a)	1.50(7)	C(8a)−N(4a)	1.31(3)
Re(1b)−Mn(1b)	3.00(1)	Re(2b)−N(2b)	2.17(3)	C(3b)−N(2b)	1.39(4)
Re(1b)−C(9b)	1.91(4)	Re(2b)−N(4b)	2.17(2)	C(4b)−C(8b)	1.40(5)
Re(1b)−C(10b)	1.93(3)	Mn(1b)−C(15b)	1.80(7)	C(4b)−N(1b)	1.41(4)
Re(1b)−C(11b)	1.95(5)	Mn(1b)−C(16b)	1.80(3)	C(4b)−N(2b)	1.31(4)
Re(1b)−N(1b)	2.15(2)	Mn(1b)−C(17b)	1.79(3)	C(5b)−C(6b)	1.34(7)
Re(1b)−N(3b)	2.19(3)	Mn(1b)−C(18b)	1.79(4)	C(5b)−N(3b)	1.40(5)
Re(2b)−Br(1b)	2.588(9)	Mn(1b)−C(19b)	1.79(3)	C(6b)−C(7b)	1.40(6)
Re(2b)−C(12b)	1.94(3)	C(1b)−C(2b)	1.26(8)	C(7b)−N(4b)	1.39(4)
Re(2b)−C(13b)	1.94(3)	C(1b)−N(1b)	1.41(4)	C(8b)−N(3b)	1.39(4)
Re(2b)−C(14b)	1.98(5)	C(2b)−C(3b)	1.30(8)	C(8b)−N(4b)	1.30(4)

Table 4. Selected Bond Angles (deg) with Estimated Standard Deviations in Parentheses

Mn(1a)−Re(1a)−C(9a)	89(2)	C(10a)−Re(1a)−N(1a)	95(1)	C(12a)−Re(2a)−C(13a)	89(2)
Mn(1a)−Re(1a)−C(10a)	85(2)	C(10a)−Re(1a)−N(3a)	170(1)	C(12a)−Re(2a)−C(14a)	91(2)
Mn(1a)−Re(1a)−C(11a)	172(1)	C(11a)−Re(1a)−N(1a)	95(2)	C(12a)−Re(2a)−N(2a)	95(1)
Mn(1a)−Re(1a)−N(1a)	92(1)	C(11a)−Re(1a)−N(3a)	94(2)	C(12a)−Re(2a)−N(4a)	171(1)
Mn(1a)−Re(1a)−N(3a)	93(1)	N(1a)−Re(1a)−N(3a)	75(1)	C(13a)−Re(2a)−C(14a)	93(2)
C(9a)−Re(1a)−C(10a)	89(2)	Br(1a)−Re(2a)−C(12a)	92(1)	C(13a)−Re(2a)−N(2a)	175(1)
C(9a)−Re(1a)−C(11a)	84(2)	Br(1a)−Re(2a)−C(13a)	91(1)	C(13a)−Re(2a)−N(4a)	98(1)
C(9a)−Re(1a)−N(1a)	175(1)	Br(1a)−Re(2a)−C(14a)	175(1)	C(14a)−Re(2a)−N(2a)	90(1)
C(9a)−Re(1a)−N(3a)	101(1)	Br(1a)−Re(2a)−N(2a)	85.1(9)	C(14a)−Re(2a)−N(4a)	94(2)
C(10a)−Re(1a)−C(11a)	90(2)	Br(1a)−Re(2a)−N(4a)	82.8(9)	N(2a)−Re(2a)−N(4a)	77.7(9)
Mn(1b)−Re(1b)−C(9b)	87(2)	C(10b)−Re(1b)−N(1b)	99(1)	C(12b)−Re(2b)−C(13b)	91(2)
Mn(1b)−Re(1b)−C(10b)	88(1)	C(10b)−Re(1b)−N(3b)	173(1)	C(12b)−Re(2b)−C(14b)	93(2)
Mn(1b)−Re(1b)−C(11b)	173(2)	C(11b)−Re(1b)−N(1b)	96(2)	C(12b)−Re(2b)−N(2b)	99(1)
Mn(1b)−Re(1b)−N(1b)	90(1)	C(11b)−Re(1b)−N(3b)	93(2)	C(12b)−Re(2b)−N(4b)	175(1)
Mn(1b)−Re(1b)−N(3b)	93(1)	N(1b)−Re(1b)−N(3b)	74(1)	C(13b)−Re(2b)−C(14b)	89(2)
C(9b)−Re(1b)−C(10b)	89(1)	Br(1b)−Re(2b)−C(12b)	94(2)	C(13b)−Re(2b)−N(2b)	169(1)
C(9b)−Re(1b)−C(11b)	87(2)	Br(1b)−Re(2b)−C(13b)	95(2)	C(13b)−Re(2b)−N(4b)	94(1)
C(9b)−Re(1b)−N(1b)	171(1)	Br(1b)−Re(2b)−C(14b)	172(1)	C(14b)−Re(2b)−N(2b)	90(2)
C(9b)−Re(1b)−N(3b)	98(1)	Br(1b)−Re(2b)−N(2b)	85(1)	C(14b)−Re(2b)−N(4b)	87(1)
C(10b)−Re(1b)−C(11b)	87(2)	Br(1b)−Re(2b)−N(4b)	85(1)	N(2b)−Re(2b)−N(4b)	75.7(9)

The ^{1}H-NMR-spectrum of the free BPYM ligand (Table 6; see Figure 1 for atom labeling) displays two sets of resonances in the aromatic region, each being readily assignable to a given pair of equivalent nuclei on the basis of expected splitting patterns. Coordination of the first metal center (MnRe or Re(Cl)(CO)$_3$) lowers the symmetry of the BPYM moiety and removes the degeneracy of each pair of protons.[18] All peaks are shifted downfield upon metal attachment by 0.33−0.49 ppm for MnRe^0/BPYM and by 0.21−0.26 ppm for Re^I(Cl)(CO)$_3$(BPYM).[18] The fact that the downfield shift is larger for MnRe^0/BPYM compared with Re^I(Cl)(CO)$_3$(BPYM) is rather surprising since it is expected that a Re^0 center will cause more shielding than a Re^I center.

Free DPP shows four sets of resonances in its ^{1}H-NMR spectrum (Table 6; see Figure 1 for atom labeling) in the aromatic region. Coordination of Re(Cl)(CO)$_3$ leads to downfield shifts of almost all proton resonances by 0.13−0.80 ppm except for those of **d′** and **e′** which have undergone an upfield shift of 0.11−0.78 ppm, respectively.[18] This unusual behavior has been interpreted in terms of a puckered conformation where the proton sticking out of the ligand plane (**e**) is predicted to show the largest downfield shift.[18] The assignment of the peaks of the MnRe/DPP compound was made according to the latter interpretation. This results in downfield shifts of most peaks by 0.02−0.98 ppm and upfield shifts for the peaks corresponding to the **d′** and **e′** protons by 0.25 and 0.56 ppm, respectively. Again, a larger downfield shift is observed upon coordination of MnRe^0 as compared with the coordination of Re^I(Cl)(CO)$_3$.

Coordination of a second metal fragment to MnRe/L leads to a further downfield shift of the proton resonances as compared with those of MnRe/L (Table 6). In MnRe^0/BPYM/Re^I, both the Re^0 and Re^I centers are coordinated to BPYM, which results in the appearance of three sets of proton resonances, indicating an asymmetric electron distribution within the BPYM ligand. It is noteworthy that this asymmetry is more pronounced (δ(**a′**) − δ(**a**) = 0.1) in both MnRe/BPYM and MnRe/BPYM/Re than in Re(Cl)(CO)$_3$(BPYM). It was shown earlier in this section that a MnRe fragment causes a larger downfield shift of the proton resonances on the site adjacent to the metal than the Re(Cl)(CO)$_3$ fragment. Therefore the doublet at 9.87 ppm is assigned to the **a′** protons and the doublet at 9.77 ppm is assigned to the **a** protons. Interestingly, the ^{1}H-NMR spectrum of MnRe/BPYM/W exhibits no distinct doublets (the same chemical shifts are found for the **a** and **a′** protons), which means that coordination of MnRe and W metal fragments does not, in this case, polarize asymmetrically the bridging BPYM ligand, most probably because of similar electron densities on the Re^0 and W^0 atoms. The ^{1}H-NMR pattern of the MnRe/DPP/Re compound was rather complex, and for the assignment of the proton resonances, use was made of the observation that a MnRe fragment causes less deshielding than a Re(Cl)(CO)$_3$ fragment. The results are summarized in Table 6.

Table 5. Selected Bond Distances and Angles in Several BPYM Complexes

structure	bond[a]	dist, Å	bond	angle, deg	ref
$[Pt(BPYM)(CN)_2]H_2O$	N(4)−C(8)	1.33(2)	C(8)−N(4)−C(7)	117.9(8)	14
	N(3)−C(8)	1.33(1)	N(3)−C(5)−C(6)	123.3(9)	
	N(2)−C(4)	1.36(1)	N(3)−C(8)−N(4)	126.1(9)	
	N(1)−C(4)	1.30(2)	C(5)−C(6)−C(7)	116.1(9)	
	C(4)−C(8)	1.50(1)	N(2)−C(4)−C(8)	114.1(7)	
			N(2)−Pt−N(4)	80.1(3)	
Cr(CO)4BPYM	N(4)−C(8)	1.340(3)	C(8)−N(4)−C(7)	116.0(2)	15
	N(3)−C(8)	1.329(4)	N(3)−C(5)−C(6)	122.4(3)	
	N(2)−C(4)	1.334(4)	N(3)−C(8)−N(4)	126.6(3)	
	N(1)−C(4)	1.325(4)	C(5)−C(6)−C(7)	118.0(3)	
	C(4)−C(8)	1.485(4)	N(2)−C(4)−C(8)	114.6(2)	
			N(2)−Cr−N(4)	75.75(9)	
$[Cu(BPYM)_2(H_2O)](PF_6)_2{\cdot}2H_2O$	N(4)−C(8)	1.345(4)	C(8)−N(4)−C(7)	118.1(3)	16
	N(3)−C(8)	1.330(4)	N(3)−C(5)−C(6)	122.9(3)	
	N(2)−C(4)	1.344(4)	N(3)−C(8)−N(4)	125.0(3)	
	N(1)−C(4)	1.324(4)	C(5)−C(6)−C(7)	117.4(4)	
	C(4)−C(8)	1.486(5)	N(2)−C(4)−C(8)	114.5(3)	
			N(2)−Cu−N(4)	80.1(1)	
[Pt(mnt)(BPYM)]·DMF	N(4)−C(8)	1.346(13)	C(8)−N(4)−C(7)	117.7(9)	17
	N(3)−C(8)	1.336(15)	N(3)−C(5)−C(6)	112.6(22)	
	N(2)−C(4)	1.380(14)	N(3)−C(8)−N(4)	125.6(10)	
	N(1)−C(4)	1.340(13)	C(5)−C(6)−C(7)	118.3(11)	
	C(4)−C(8)	1.450(15)	N(2)−C(4)−C(8)	115.5(9)	
			N(2)−Pt−N(4)	79.7(3)	
MnRe/BPYM/Re	N(4a)−C(8a)	1.31(3)	C(8a)−N(4a)−C(7a)	110(3)	
	N(3a)−C(8a)	1.40(4)	N(3a)−C(5a)−C(6a)	116(3)	
	N(2a)−C(4a)	1.30(4)	N(3a)−C(8a)−N(4a)	126(3)	
	N(1a)−C(4a)	1.40(4)	C(5a)−C(6a)−C(7a)	116(3)	
	C(4a)−C(8a)	1.50(4)	N(2a)−C(4a)−C(8a)	119(2)	
			N(2a)−Re(2a)−N(4a)	77.7(9)	
			N(1a)−Re(1a)−N(3a)	75(1)	
	N(4b)−C(8b)	1.30(4)	C(8b)−N(4b)−C(7b)	120(3)	
	N(3b)−C(8b)	1.39(4)	N(3b)−C(5b)−C(6b)	117(5)	
	N(2b)−C(4b)	1.31(4)	N(3b)−C(8b)−N(4b)	120(3)	
	N(1b)−C(4b)	1.41(4)	C(5b)−C(6b)−C(7b)	121(4)	
	C(4b)−C(8b)	1.40(5)	N(2b)−C(4b)−C(8b)	115(3)	
			N(2b)−Re(2b)−N(4b)	75.7(9)	
			N(1b)−Re(1b)−N(3b)	74(1)	

[a] The bonds are numbered in the same way as for MnRe/BPYM/Re. In the mononuclear complexes, N(2) and N(4) are coordinated to the metal center.

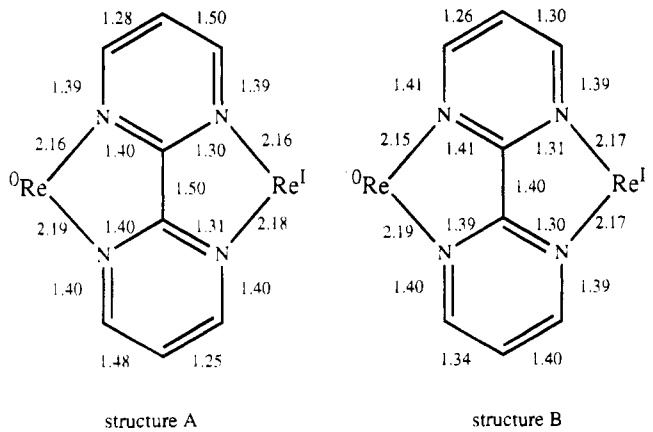

structure A structure B

Figure 3. Selected bond distances (Å) of the two independent molecules MnRe/BPYM/Re.

In principle, two isomeric structures are possible for the MnRe/L/Re complexes. One isomer has the $Mn(CO)_5$ fragment and Br^- cis to each other; in the other isomer these groups are positioned trans to each other. It can be expected that both isomers show different ^{1}H-NMR patterns. However, in the ^{1}H-NMR spectra of both the BPYM and DPP complexes, only one isomer was observed. According to the X-ray structure of the BPYM compound, it is concluded that in the solution we are also dealing with the trans isomers, $Mn(CO)_5$ and Br^- lying on different sides of the plane defined by the ligand L; see Figure 2.

Electronic Absorption and Resonance Raman Spectra. The UV/vis spectral data for the complexes in three different solvents are collected in Table 7, and the spectra of MnRe/L, MnRe/L/Re, and MnRe/BPYM/W are presented in Figure 4. The absorption bands are rather intense and solvatochromic. This indicates that they belong to MLCT transitions to the lowest π^* orbital(s) of BPYM or DPP, in agreement with previous assignments for $Re(Cl)(CO)_3(L)$ and $Re(Cl)(CO)_3(L)Re(Cl)(CO)_3$ complexes.[8,11,12,18]

The lowest-energy absorption band of the dinuclear MnRe/L complexes is therefore assigned to MLCT transitions from the Re^0 atom of the dinuclear unit to the π^* LUMO orbital of the ligand L. The lowest-energy band of the trinuclear MnRe/L/Re species occurs at much lower energies than the MLCT absorption bands[8,11,12,18] of analogous $Re(Cl)(CO)_3(L)Re(Cl)(CO)_3$ complexes in which the ligand (L = BPYM or DPP) bridges between two Re^I atoms. This comparison indicates that the first absorption band of MnRe/L/Re still corresponds to MLCT transitions from the $MnRe^0$ fragment to the π^* LUMO of the bridging ligand L. Inspection of Table 7 and Figure 4 clearly shows that coordination of a mononuclear metal fragment $Re(Br)(CO)_3$ to a MnRe/L unit to form the trinuclear MnRe/L/Re complex causes a significant red shift of these $MnRe^0 \rightarrow$ L MLCT transitions with respect to those of the dinuclear

Table 6. ^{1}H-NMR and IR Data for the BPYM and DPP Compounds

compound	chem shift, ppm[a]		ν(CO), cm^{-1} [b]
BPYM		**a** 8.98 (d, 4H, 4.6 Hz) **b** 7.60 (t, 2H, 4.6 Hz)	
Re(Cl)(CO)$_3$(BPYM)[18]	**a'** 9.24 (d, 2H, 5.0 Hz)	**a** 9.23 (d, 2H, 4 Hz) **b** 7.81 (t, 2H, 5 Hz)	2025, 1926 m, 1903 m
MnRe/BPYM	**a'** 9.47 (d, 2H)	**a** 9.31 (d, 2H) **b** 7.95 (t, 2H)	2056 m, 2001 s, 1949 vs, 1901 m
MnRe/BPYM/Re[c]	**a'** 9.87 (d, 2H)	**a** 9.77 (d, 2H) **b** 8.28 (t, 2H)	2060 m, 2030 s, 2007 s, 1958 m, 1936 m, 1917 m
MnRe/BPYM/W	**a'** 9.61 (m, 2H)	**a** 9.61 (m, 2H) **b** 8.00 (t, 2H)	2058 m, 2013 m, 2004 s, 1956 s, 1912 s, 1855 m
MnRe/BPYM/W[d]			2060 m, 2024 m, 2005 s, 1969 m, 1950 m, 1923 s, br, 1896 s, 1884 sh, 1869 s, 1826 m, br
W/BPYM/W[e,27]			2028 w
DPP		**a** 8.72 (s, 2H) **b** 8.23 (d, 2H, 4.3 Hz) **c** 7.31 (dd, 2H) **d,e** 7.90 (d, 4H)	
Re(Cl)(CO)$_3$(DPP)[18]	**a'** 9.07 (d, 1H, 3 Hz) **b'** 9.03 (d, 1H, 5.4 Hz) **c'** 7.55 (dd, 1H) **d'** 7.79 (td, 1H, 1.2 Hz, 8 Hz) **e'** 7.12 (d, 1H, 9 Hz)	**a** 8.85 (d, 1H, 3 Hz) **b** 8.64 (d, 1H, 4.8 Hz) **c** 7.71 (m, 1H) **d** 8.21 (td, 1H, 1.2 Hz, 8 Hz) **e** 8.04 (d, 1H, 8 Hz)	2023 s, 1925 m, 1904 m
MnRe/DPP	**a'** 9.30 (d, 1H) **b'** 9.21 (d, 1H) **c'** 7.65 (m, 1H) **d'** 7.65 (m, 1H) **e'** 7.34 (d, 1H)	**a** 8.86 (d, 1H) **b** 8.70 (d, 1H) **c** 7.65 (m, 1H) **d** 8.19 (td, 1H) **e** 7.92 (d, 1H)	2055 m, 2000 s, 1952 vs, 1901 m
MnRe/DPP/Re	**a'** 9.29 (m, 1H) **b'** 9.29 (m, 1H) **c'** 7 .91 (dt, 1H, 6 Hz) **d'** 8.21 (dt, 1H, 9.5 Hz) **e'** 8.65 (d, 1H, 9.5 Hz)	**a** 9.29 (m, 1H) **b** 9.11 (d, 1H, 4 Hz) **c** 7.91 (dt, 1H, 4 Hz) **d** 8.21 (dt, 1H, 7 Hz) **e** 8.81 (d, 1H, 7 Hz)	2057 m, 2024 s, 2001 s, 1957 m, 1933 m, 1909 m

[a] Recorded in acetone-d6 on a Bruker AC 100. [b] Measured in THF; this work. [c] Measured on an AMX 300 in acetone-d_6; note that the chemical shifts are shifted approximately 0.1 ppm downfield compared to those of the spectra recorded on the Bruker AC 100 spectrometer. [d] Measured in KBr. [e] rR spectrum in acetonitrile.

Table 7. UV/Vis Data (λ_{max} in nm; $\epsilon \times 10^{-3}$ in M^{-1} cm^{-1} in Parentheses) for MnRe/L, MnRe/L/W, and MnRe/L/Re (L = BPYM, DPP) at Room Temperature

compound	toluene	THF	acetonitrile	KBr
MnRe/BPYM	553	523 (3.8)	511	
	411	392 (4.0)	382	
		280 (sh) (> 10^4)		
MnRe/DPP	583	557 (6.5)	555	
			310 (sh)	
			280 (> 10^4)	
MnRe/BPYM/Re[a]		671 (3.6)	664	739
		473 (4.8)	469	501
		380 (4.6)	364	384 (sh)
		300 (sh)		
MnRe/BPYM/W	751	684 (5.1)	655	721
	680 (sh)	628 (sh)	616 (sh)	660
	473	450 (8.9)	435	469
		388 (6.0)	384 (sh)	381
			288 (sh)	288 (sh)
MnRe/DPP/Re	670	636 (9.7)	624	656
	485	474 (6.5)	447	466
	317	320 (22)	328	331

[a] Insoluble in toluene.

MnRe/L complex. This spectral shift is paralleled by a positive shift of the reduction potentials[40] of the bridging ligand. For BPYM, the MLCT band maximum shifts by −4510 cm^{-1} (in CH_3CN) and the reduction potential by +0.62 V (i.e. 5000 cm^{-1}). Somewhat smaller shifts were found for DPP: −1990 cm^{-1} (in CH_3CN), +0.39 V (i.e. 3150 cm^{-1}). The magnitudes of these spectral and electrochemical shifts are comparable with those observed for other diimine-bridged bimetallic complexes, irrespective of the detailed nature of the metal fragments.[8,9,11,12,18-28] They indicate a significant stabilization of the π^* LUMO orbital of the bridging ligand upon formation of the MnRe/L/Re complexes.

The MnRe/BPYM/W complex exhibits a broad absorption band with a maximum at 684 nm and a shoulder at about 630 nm (in THF); see Table 7 and Figure 4A. This is the same wavelength range where the MnRe^0 → BPYM and W^0 → BPYM MLCT transitions occur in the MnRe/L/Re and (CO)$_4$W(BPYM)W(CO)$_4$[27] complexes, respectively. Apparently, the lowest-energy band of MnRe/BPYM/W encompasses both the MnRe^0 → BPYM and W^0 → BPYM MLCT transitions. This conclusion is supported by the observation of two well-developed absorption maxima at 584 and 634 nm in the spectrum measured in a 2-MeTHF glass at 80 K. Characteristic of MLCT absorptions, both bands occur at higher energies in the rigid glass as compared with the fluid solution.

All trinuclear complexes under study exhibit a second intense solvatochromic band at higher energies. The first band being assigned to charge-transfer transitions from the MnRe^0 unit to the π^* LUMO of the bridging ligand L, the higher-energy band of MnRe/L/Re should belong to MLCT transitions from the Re^I atom of the Re(Br)(CO)$_3$ fragment to the same π^* LUMO. Alternatively, it may be assigned to MLCT transitions originating from the MnRe^0 fragment but directed to the second unoccupied (SLUMO) π^* orbital of the bridging ligand L. In fact, the two lowest empty π^* orbitals are known to be rather close in energy in both BPYM-[27] and DPP-bridged[41] complexes and transitions to both of them are symmetry-allowed. In order

(40) (a) van Outersterp, J. W. M.; Hartl, F.; Stufkens, D. J. *Organometallics* **1995**, *14*, 3303. (b) van Outersterp, J. W. M.; Hartl, F.; Stufkens, D. J. *Inorg. Chem.* **1994**, *33*, 2711.

(41) Záliš, S.; Vlček Jr., A. Unpublished results of MNDO calculations.

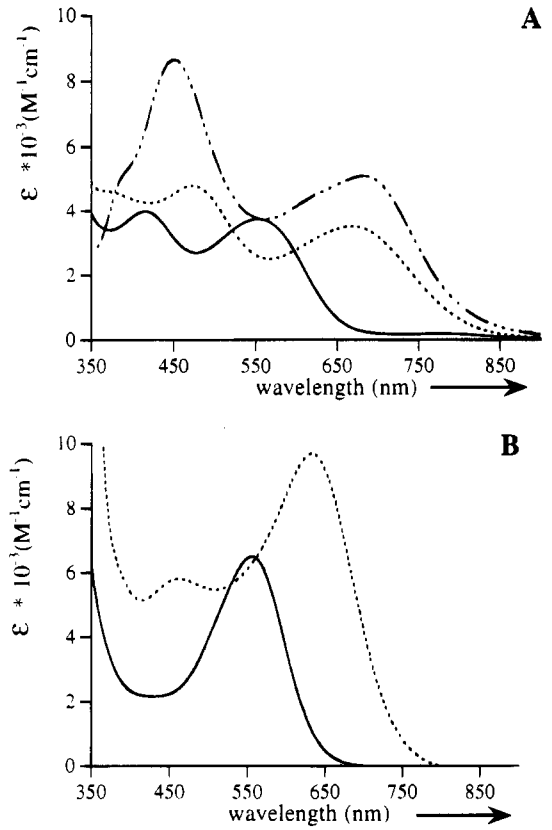

Figure 4. UV/vis spectra (measured in THF): (A) MnRe/BPYM (—), MnRe/BPYM/Re (···) and MnRe/BPYM/W (—···—); (B) MnRe/DPP (—), MnRe/DPP/Re (···).

Table 8. Resonantly Enhanced Raman Bands (cm^{-1}) of the Trinuclear Complexes MnRe/L/Re and MnRe/BPYM/W

MnRe/BPYM/Re		MnRe/BPYM/W		MnRe/DPP/Re	
λ_{exc} 458 nm	λ_{exc} 655 nm	λ_{exc} 488 nm	λ_{exc} 648 nm	λ_{exc} 458 nm	λ_{exc} 608 nm
2064	2066	2060	2060		2059
2029		2024	2024	2028	2028
		2006			
	1572				
1559		1557	1557	1573	1573
	1549	1545	1545	1563	1563
1487		1466	1466	1487	1487
	1477			1477	1477
1336	1336	1332		1359	
1199	1199	1181	1181	1345	
		1031	1031	1275	1276

to solve this problem and to obtain more detailed information on the nature of the MLCT states of the trinuclear MnRe/L/Re and MnRe/BPYM/W complexes, we have investigated their resonance Raman (rR) spectra.

For the trinuclear complexes under study, the Raman spectra could be measured by dispersing the complexes in a KNO_3 pellet and rotating it at room temperature during the rR experiment. It was, however, very difficult to obtain high-quality Raman spectra for MnRe/DPP/Re because of photodecomposition. Spectra were recorded with laser lines varying from 458 to 655 nm, exciting thus into both absorption bands. For all complexes investigated, the most strongly enhanced Raman bands occur in the 1000–1600 cm^{-1} region (Table 8; Figures 5 and 7). They belong to internal vibrations of the bridging ligand, which means that the resonant electronic transitions involved are localized at, or directed to, this ligand. Since intraligand electronic transitions of both BPYM and DPP occur at much higher energy,[12] these rR effects are ascribed to vibronic couplings to

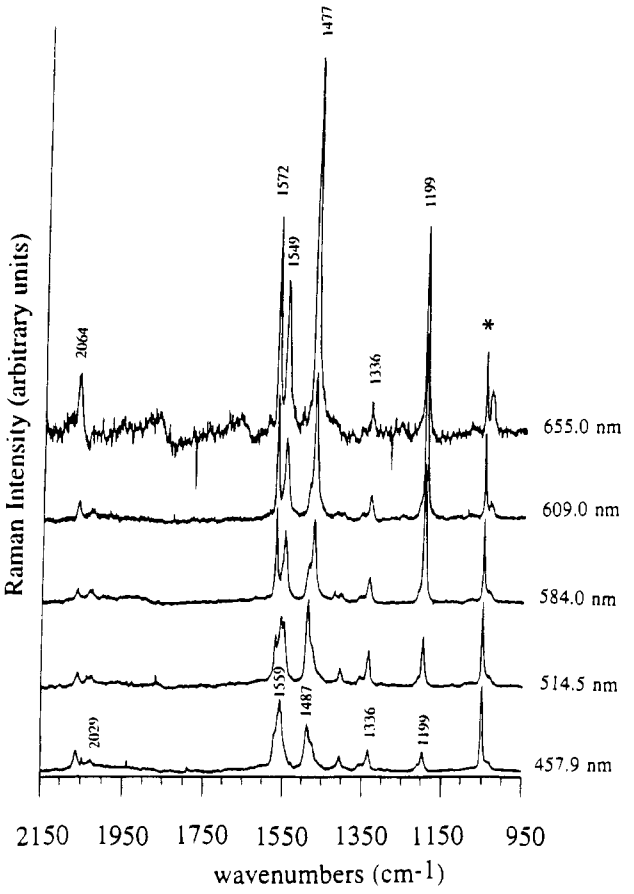

Figure 5. Resonance Raman spectra of MnRe/BPYM/Re in KNO_3 (*) at room temperature and at different excitation wavelengths.

MLCT transitions directed to these ligands, in accord with the assignment of both visible absorption bands discussed above.

The rR spectra of MnRe/BPYM/Re are presented in Figure 5. Upon excitation with $\lambda = 655$ nm into the first absorption band, a rR effect is observed for a band at 2064 cm^{-1}, which is assigned to a symmetrical CO-stretching vibration of the $(CO)_5MnRe(CO)_3$ fragment. This assignment is based on a comparison of the IR spectra of MnRe/BPYM, Re/BPYM, and MnRe/BPYM/Re (Table 6). The IR spectrum of the last complex is nearly a superposition of those of the former two complexes. There is only a very small shift of the ν(CO) vibrations to higher frequencies caused by the decreasing basicity of BPYM upon bridge formation. Thus, the highest IR frequency of MnRe/BPYM at 2056 cm^{-1} shifts to 2060 cm^{-1} in MnRe/BPYM/Re and to 2058 cm^{-1} in MnRe/BPYM/W.

The observation of a rR effect only for this CO stretching mode implies that the electronic transitions involved in the lowest-energy absorption band originate from the $Re^0(d_\pi)$ orbitals of the $(CO)_5MnRe(CO)_3$ fragment. Resonant enhancement of this Raman band has been observed for $(CO)_5MM'(CO)_3$(α-diimine) (M, M′ = Mn, Re) complexes.[37] As the d_π orbitals are involved in the $MnRe^0 \rightarrow CO$ π-back-bonding, their depopulation by MLCT excitation affects the CO bonds and gives rise to the rR effect on the ν(CO) vibration.

When excitation takes place into the higher-energy absorption band of MnRe/BPYM/Re ($\lambda \leq 584$ nm), the rR effect of the 2064 cm^{-1} band is weaker and a second, weak, Raman band appears at 2029 cm^{-1}. By comparing again the IR spectra of MnRe/BPYM, Re/BPYM, and MnRe/BPYM/Re (Table 6), we can assign this band to a symmetrical CO-stretching mode of the $Re^I(Br)(CO)_3$ fragment of MnRe/BPYM/Re. The weakness of the rR effect for this vibration is not unexpected since recent

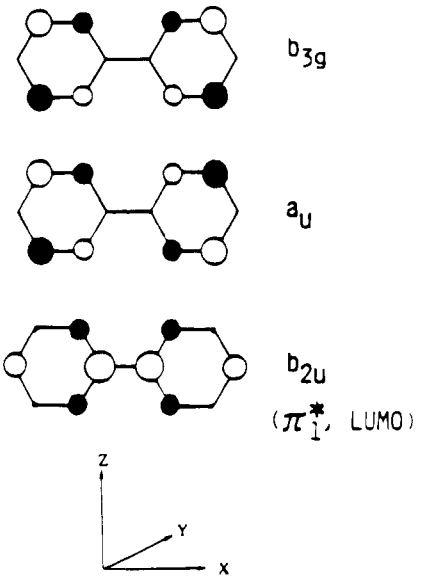

Figure 6. Low-lying unoccupied π^* molecular orbitals of BPYM.[27]

rR studies have shown that charge-transfer transitions of halide complexes such as $Re(X)(CO)_3$(pTol-DAB) (X = halide; pTol-DAB = di-*p*-tolyl-1,4-diaza-1,3-butadiene)[42] and $Ru(X)(R)(CO)_2$(α-diimine) (X = halide, R = alkyl, α-diimine = diisopropyl-1,4-diaza-1,3-butadiene, pyridine-2-carbaldehyde *N*-isopropylimine, 2,2′-bipyridine)[43] always give rise to only very weak (if any) resonant enhancement of the Raman band corresponding to the symmetrical CO vibration. This is caused by the admixture of the p_π orbitals of X to the $Re(d_\pi)$ orbitals, which changes the CT character of the electronic transitions and diminishes the effect of CT excitation on the Re → CO π-back-bonding and, hence, on the CO bonds. Quite recently, the same ν(CO) frequency was observed as a very weak Raman band at 2023 cm^{-1} in the surface enhanced raman scattering (SERS) spectra of $Re(Br)(CO)_3$(BPYM).[47]

The above results show that the first absorption band belongs to MLCT transitions from the $(CO)_5MnRe(CO)_3$ fragment only. The second band is dominated by CT transitions originating from the $Re^I(Br)(CO)_3$ fragment with a minor contribution of the transitions from the $MnRe^0$ fragment. Previous theoretical[9] and absorption spectral[27,28] studies of mono- and dinuclear BPYM complexes have shown that the MLCT transitions involve the π^* orbitals of b_{2u} and a_u symmetries (within the D_{2h} local point group of the ligand), shown in Figure 6. As the b_{2u} is bonding with respect to the C−C bond connecting the two pyrimidine rings of the BPYM ligand, its occupation by MLCT excitation will be accompanied by a strengthening of the inter-ring C−C bond. This will give rise to resonance enhancement of the intensity of the Raman band that corresponds to the inter-ring C−C stretching vibration. Occupation of the a_u orbital will, on the other hand, hardly affect the inter-ring C−C bond and will therefore not be accompanied by a rR effect for the inter-ring stretch which is expected at about 1330 cm^{-1}.[27,44-45] The rR spectra of MnRe/BPYM/Re (Figure 5) show that a band at 1336 cm^{-1} is resonantly enhanced by excitation into both absorption bands. This means that the

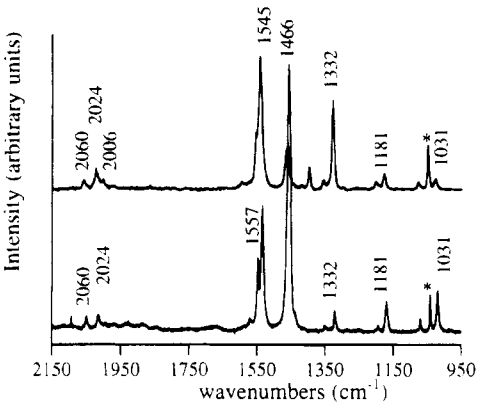

Figure 7. Resonance Raman spectra of MnRe/BPYM/W in KNO_3 (*) at room temperature. Excitation wavelength: 488 nm (top); 648 nm (bottom).

MLCT transitions from both metal fragments are directed to this $\pi^*(b_{2u})$ orbital. The low-energy band thus belongs to the $MnRe^0(d_\pi) \rightarrow \pi^*(b_{2u})$ transitions, and the higher-energy one to the $Re^I(d_\pi) \rightarrow \pi^*(b_{2u})$ transitions. It cannot, however, be completely excluded that weaker transitions to $\pi^*(a_u)$ also contribute to these bands.

A similar assignment has been presented for the two absorption bands of $[Mo(CO)_4(BPYM)Ru(bpy)_2](PF_6)_2$[28a] and $Mo(CO)_4(BPYM)Re(Cl)(CO)_3$,[28b] in which BPYM also bridges between metals in different oxidation states. Matheis et al.[28] assigned the first absorption band of the former complex to $Mo(d_\pi) \rightarrow \pi^*(b_{2u})$ transitions and the second, composite, band to $Ru(d_\pi) \rightarrow \pi^*(b_{2u})$, $Mo(d_\pi) \rightarrow \pi^*(a_u)$ and $Ru(d_\pi) \rightarrow \pi^*(a_u)$ transitions.

There is no evidence for a strong electronic interaction between the two Re centers of MnRe/BPYM/Re, and the two metal fragments seem to behave independently with respect to their electronic transitions and molecular vibrations. This becomes even more evident when we consider the rR behavior of the BPYM vibrations between 1400 and 1600 cm^{-1} which are assigned[44-45] to coupled C−H bending, C−C stretching, and C−N stretching vibrations. Figure 5 shows that BPYM vibrations at 1572, 1549, and 1477 cm^{-1} are enhanced in resonance with the $MnRe^0(d_\pi) \rightarrow \pi^*(b_{2u})$ transitions of the first absorption band, whereas those at 1559 and 1487 cm^{-1} are in resonance with the $Re^I(d_\pi) \rightarrow \pi^*(b_{2u})$ transitions. As far as we know, this is the first time that different ligand vibrations are found to be vibronically coupled to electronic transitions directed to the same ligand orbital ($\pi^*(b_{2u})$). In the next section, this remarkable result will be discussed in relationship to the X-ray and ^{1}H-NMR data.

A completely different behavior is observed for the complexes MnRe/BPYM/W and MnRe/DPP/Re. The absorption spectrum of MnRe/BPYM/W shows again two absorption bands (Figure 4A, Table 7). The rR spectra obtained by excitation into either of these bands exhibit resonance enhancement of intensity for Raman bands at 2060, 2024, and 2006 cm^{-1} (Figure 7). The bands at 2060 and 2006 cm^{-1} belong to vibrations of the $(CO)_5MnRe(CO)_3$ fragment; the 2024 cm^{-1} band belongs to a ν_s(CO) vibration of the $W(CO)_4$ moiety (Table 6). Apparently, MLCT transitions from both metal fragments are involved in the two absorption bands of this complex. This is not surprising, since, contrary to the Re^0 and Re^I d orbitals of the MnRe/BPYM/Re complex, the Re^0 and W^0 d_π orbitals would hardly differ in energy. As a result, MLCT transitions to BPYM from the d_π orbitals of both metal fragments (Re^0, W^0) are expected to (nearly) coincide. Hence, the electronic transitions involved in the two MLCT bands have to differ in the nature of the final

(42) Stor, G. J.; Stufkens, D. J.; Oskam, A. *Inorg. Chem.* **1992**, *31*, 1318.
(43) Nieuwenhuis, H. A.; Stufkens, D. J.; Oskam, A. *Inorg. Chem.*, in press.
(44) Neto, N.; Sbrana, G.; Muniz-Miranda, M. *Spectrochim. Acta* **1990**, *46A*, 705.
(45) Sbrana, G.; Neto, N.; Muniz-Miranda, M.; Nocentini, M. *J. Phys. Chem.* **1990**, *94*, 3706.
(46) van Outersterp, J. W. M.; et al. Unpublished results.
(47) Vlčková, B.; Matějka, P.; van Outersterp, J. W. M.; Snoeck, Th. L.; Stufkens, D. J. *Inorg. Chem.* **1994**, *33*, 2132.

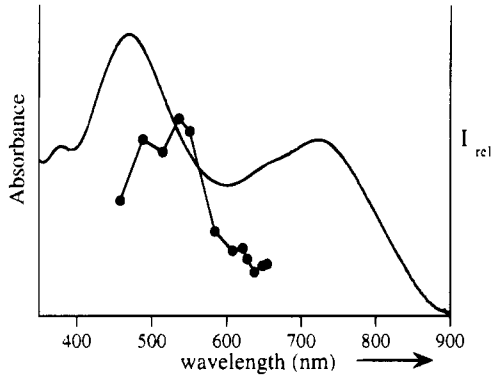

Figure 8. Resonance Raman excitation profile for the ν_s(C−C) inter-ring vibration (1332 cm^{-1}) of MnRe/BPYM/W. The intensities were measured relative to the intensity of the 1051 cm^{-1} band of KNO_3.

optical orbital. The transitions to $\pi^*(b_{2u})$ are expected to be more intense than those directed to $\pi^*(a_u)$ because of the more favorable overlap with the d_π orbitals.[27] The higher-energy absorption band at 450 nm is therefore assigned to the d_π (Re^0,W^0) → b_{2u} transitions; the low-energy band at 751 nm to the d_π(Re^0,W^0) → a_u transitions. This assignment is rather surprising, as it implies a reversal of b_{2u} and a_u orbital energies compared with those of both the free ligand and the MnRe/BPYM and MnRe/BPYM/Re complexes. This unusual assignment is supported by the much stronger rR effect for the 1332 cm^{-1} vibration of MnRe/BPYM/W upon excitation into the higher-energy absorption band than into the lower-energy band as manifested by the excitation profile of the 1332 cm^{-1} Raman band; see Figure 8. The same effect was recently found for $\{W(CO)_4\}_2$(BPYM).[27] Also for this compound, the second absorption band was more intense than the first one and the inter-ring C−C stretching vibration was only enhanced when excitation took place into the second band.[27] The reversal of the b_{2u} and a_u orbitals, found for MnRe/BPYM/W, but not for MnRe/BPYM/Re, is most probably caused by the π-back-donation to the b_{2u} BPYM orbital that is expected to be much stronger from the $W^0(CO)_4$ than $Re^I(Br)(CO)_3$ fragment. For symmetry reasons (see Figure 6), the b_{2u} BPYM orbital overlaps with the metal d_π orbital much better than the a_u orbital. Hence, strong W^0 → BPYM π-back-bonding would destabilize the b_{2u} orbitals relative to a_u. Sufficiently strong π-interaction would reverse the orbital order. Contrary to the rR spectra of MnRe/BPYM/Re, the same BPYM vibrations in the 1400−1600 cm^{-1} region are resonance enhanced throughout the two absorption bands of MnRe/BPYM/W, which means that this ligand has retained its symmetric structure in this complex.

In the case of MnRe/DPP/Re, a rR effect for ν_s(CO) of the $Re(Br)(CO)_3$ fragment at 2028 cm^{-1} was only observed upon excitation into the higher-energy absorption band (Table 8). This Raman band gradually disappeared upon going to longer-wavelength excitation and the 2059 cm^{-1} band belonging to ν_s(CO) of the $(CO)_5MnRe(CO)_3$ fragment appeared when excitation became directed into the first absorption band. Although the Raman spectra could only be excited at the high-energy side of this band because of increasing photodecomposition, it could still be concluded that, just as for MnRe/BPYM/Re, the low-energy absorption band of this DPP complex belongs to MLCT transitions from $MnRe^0$, the higher one to the corresponding transitions from Re^I. However, contrary to those of the corresponding BPYM complex, the same Raman bands of DPP were resonance enhanced upon excitation into both absorption bands, which means that the DPP ligand is not significantly distorted when it bridges between metals in different oxidation states.

Asymmetric Distortion of the Bridging BPYM Ligand. The molecular structure of the MnRe/BPYM/Re complex (Figure 3) clearly points to a distortion of the BPYM ligand with respect to the plane that bisects the pyrimidine rings. Notably, the C(4)−N and C(8)−N bonds adjacent to the Re^0 atom of the $(CO)_5MnRe(CO)_3$ fragment are significantly longer than the corresponding bonds adjacent to the Re^I atom of $Re(Br)(CO)_3$ (C(4) and C(8) are the carbon atoms connecting the two pyrimidine rings). This observation is in accord with a stronger $MnRe^0$ → BPYM than Re^I → BPYM π-back-donation that is directed to the original b_{2u} LUMO of the BPYM ligand. The C−N bonds are affected by the population of the b_{2u} orbital because of its π^*-antibonding nature; see Figure 6. However, the nonequivalence of these bonds indicates that (i) the electronic interaction between the two Re atoms is rather weak, maintaining their different formal oxidation states, and (ii) the π-system of the BPYM ligands is no longer fully delocalized. The asymmetric electron distribution within the BPYM ligand is also evident from the ^{1}H-NMR spectra which show a 0.1 ppm difference in the chemical shifts of the protons bound at the **a′** and **a** positions.

The most intriguing evidence for the bonding asymmetry of the bridging BPYM ligand in MnRe/BPYM/Re comes from the rR spectra. As shown above, this complex exhibits an absorption band in the red spectral region that corresponds predominantly to the $MnRe^0$ → BPYM transitions, whereas the band at higher energy is due to the Re^I → BPYM MLCT transitions. The Raman spectra excited in resonance with the $MnRe^0$ → BPYM transitions show enhancement of intensity for the bands at 1549 and 1477 cm^{-1}, which correspond[27,44,45] to B_{3u} and A_g vibrations of free BPYM, respectively. (Note that B_{3u} transforms as A_1 and A' in C_{2v} and C_s symmetries, respectively.) The A_g and B_{3u} coupled normal modes contain[44,45] a contribution from stretchings of the C(1),C(3),C(5),C(7)−N and C(4),C(8)−N bonds, respectively. When the exciting laser line approaches the higher Re^I → BPYM MLCT absorption band, the intensities of these Raman bands decrease and new bands, presumably corresponding to the same type of vibrations, appear at 1559 and 1487 cm^{-1}. Taking into account that these vibrational modes contain significant contribution from C(4),C(8)−N bond stretchings,[44,45] we may conclude that this effect again points to the nonequivalence of the C(4),C(8)−N(Re^0) and C(4),C(8)−N(Re^I) bonds within the BPYM ligand. Moreover, the fact that the Raman intensity corresponding to each of these two different sets of local vibrations is enhanced in resonance with a different MLCT transition suggests that the two MLCT excited states involved are localized within the chelate rings adjacent to the metal center from which the MLCT transitions originate. Thus, the low-energy $MnRe^0$ → BPYM transition affects mainly the N(1)−C(4)−C(8)−N(3) part of the BPYM ligand whereas the Re^I → BPYM transition at higher energy is localized mainly in its N(2)−C(4)−C(8)−N(4) part. Consequently, the MLCT transitions from the $MnRe^0$ and Re^I centers are vibronically coupled to different local modes of the asymmetrically distorted BPYM ligand, giving rise to the observed dependence of corresponding Raman frequencies on the excitation wavelength.

Another interesting observation is that the Raman band at 1572 cm^{-1} is strongly enhanced upon excitation into the low-energy $MnRe^0$ → BPYM transition. Up to now, a rR effect of this band was observed for the asymmetric complexes $W(CO)_4$BPYM, $[W(CO)_4BPYM]^{-}$, and $Ru(BPYM)_3^{2+}$ but not for the symmetric complexes $(CO)_4M(BPYM)M(CO)_4$ (M = Mo, W).[27] This Raman band belongs most probably[44,45] to the A_g vibration of BPYM which has a strong contribution from C(1),C(3),C(5),C(7)−N stretchings. The bonding asymmetry

of the bridging BPYM ligand in MnRe/BPYM/Re appears to be a consequence of only a very weak electronic interaction between the $(CO)_5MnRe^0(CO)_3$ and $Re^I(Br)(CO)_3$ metal fragments through the BPYM bridge. The limited extent of the metal−metal interaction is clearly manifested by the presence of two, experimentally distinguishable, $MnRe^0 \rightarrow$ BPYM and $Re^I \rightarrow$ BPYM localized MLCT transitions. Thus, both Re atoms render their original formal oxidation states, i.e. Re^0 and Re^I, unchanged and MnRe/BPYM/Re may be viewed as a class II[48] mixed-valence compound. Hence, the BPYM ligand experiences simultaneous bonding to two different metal centers with rather different σ-acceptor and, especially, π-donor properties. The inability of BPYM to level out these differences by a strong interaction with both metal centers results in its asymmetric distortion. It is quite conceivable that the distortion of the bridging BPYM ligand in heterobinuclear complexes might be a more general effect and a way to design and control the BPYM-mediated metal−metal interaction in polynuclear supramolecular compounds.

There is already some evidence that such a distortion of BPYM is not restricted to the complex MnRe/BPYM/Re. A similar effect was quite recently observed by us for the polynuclear complex $Os_3(CO)_{10}(BPYM)Re(Br)(CO)_3$, in which the $Os_3(CO)_{10}$ moiety has replaced the $(CO)_5MnRe(CO)_3$ fragment in MnRe/BPYM/Re.[46] Moreover, surface enhanced raman scattering (SERS) of the complex $Re(Br)(CO)_3(BPYM)$ dissolved in DMSO together with an aqueous Ag colloid also showed additional Raman bands upon changing the excitiation wavelength from 514.5 to 569 nm.[47] This effect is most likely due to the formation of Ag_n^+−BPYM−$Re(Br)(CO)_3$ in which BPYM is again asymmetrically distorted.

Such a bonding asymmetry of the BPYM ligand was not observed for the MnRe/BPYM/W complex. Its ^{1}H-NMR spectrum shows that the protons at the **a** and **a′** positions have the same chemical shifts. The resonance Raman spectra show a rR effect for the same BPYM Raman bands, especially those at 1545 and 1466 cm^{-1}, regardless the excitation wavelength. These vibrations most probably correspond again to the B_{3u} and A_g modes, respectively. The band at 1572 cm^{-1} is not resonantly enhanced. The absence of a distortion in MnRe/BPYM/W does not, however, necessarily imply any strong electronic interaction between the $MnRe^0$ and W^0 centers mediated by the BPYM bridge. It may be explained by the similarity of the bonding properties of the $(CO)_5MnRe(CO)_3$ and $W(CO)_4$ metal fragments, both Re^0 and W^0 atoms being in the same formal oxidation state. Interestingly, the positive shift of the potential of the BPYM ligand-localized reduction in MnRe/BPYM is much smaller (+480 mV) upon formation of the MnRe/BPYM/W ($E_{1/2} = -1.01$ V vs Fc/Fc^+ in *n*-PrCN at room temperature) complex than of the MnRe/BPYM/Re complex (+620 mV). This observation is fully in line with the above explanation as it shows that the $W(CO)_4$ fragment is both a weaker σ-acceptor and stronger π-donor than $Re(Br)(CO)_3$.

The bridging DPP ligand in MnRe/DPP/Re does not exhibit any asymmetry of the pyrazine ring, as manifested by identical chemical shifts of the protons at the **a** and **a′** positions (see Figure 1). Moreover, the same Raman bands of the DPP bridge are resonantly enhanced upon excitation into both absorption bands. However, the pyridine rings of the DPP ligand in MnRe/DPP/Re are nonequivalent, as shown by different chemical shifts exhibited by the protons at the **b** and **b′** as well as at the **e** and **e′** positions, in accord with the formulation of $MnRe^0/DPP/Re^I$ as a class II mixed-valence complex with only weakly interacting $MnRe^0$ and Re^I metal centers. For steric reasons, the two pyridine rings of the DPP ligand are tilted away from the Re^0−(pyrazine ring)−Re^I plane by as much as 30°,[23] strongly weakening the conjugation between the pyridine and pyrazine parts of the DPP ligand.[23,41] Hence, the two pyridine rings are electronically rather isolated and nonequivalent, as each of them interacts with a different metal center. On the other hand, the $MnRe^0$−Re^I coupling through the pyrazine ring of the DPP bridge is strong enough to attain a uniform distribution of electron density over the symmetrically nonequivalent carbon atoms **a** and **a′**. Apparently, the electronic coupling between the two Re atoms is stronger through the pyrazine ring of DPP than through the pyrimidine rings of BPYM. Bridging DPP has already been shown to provide stronger metal−metal electronic coupling than BPYM, especially in those complexes where the coupling is dominated by the π-back-donation from the metal d_π orbitals to the π^* orbital(s) of the bridging ligand.[21,22,48,49]

Acknowledgment. The Netherlands Foundation for Chemical Research (SON) and the Netherlands Organisation for Pure Research (NWO) are thanked for financial support. A.V. acknowledges financial support from the Granting Agency of the Czech Republic (Grant No. 203/93/0250).

Supporting Information Available: Listings of the fractional coordinates and isotropic thermal parameters of the hydrogen atoms, anisotropic thermal parameters, bond distances, and bond angles (6 pages). Ordering information is given on any current masthead page.

IC9414482

(48) Robin, M. B.; Day, P. *Advances in Inorganic Chemistry and Radiochemistry*; Academic Press: New York and London, 1967.

(49) Ruminski, R. R.; Cockroft, T.; Shoup, M. *Inorg. Chem.* **1988**, *27*, 4026.